

# Dissection of Functional Domains of the Voltage-Dependent $\text{Ca}^{2+}$ Channel $\alpha_2\delta$ Subunit

Ricardo Felix,<sup>1</sup> Christina A. Gurnett,<sup>1</sup> Michel De Waard,<sup>2</sup> and Kevin P. Campbell<sup>1</sup>

<sup>1</sup>Howard Hughes Medical Institute, Department of Physiology and Biophysics, University of Iowa College of Medicine, Iowa City, Iowa 52242, and <sup>2</sup>Institut National de la Santé et de la Recherche Médicale U464, Institut Jean Roche, Faculté de Médecine Nord, 13916 Marseille 20, France

Coexpression of the cloned voltage-dependent  $\text{Ca}^{2+}$  channel  $\alpha_2\delta$  subunit with the pore-forming  $\alpha_1$  subunit results in a significant increase in macroscopic current amplitude. To gain insight into the mechanism underlying this interaction, we have examined the regulatory effect of either the  $\alpha_2\delta$  complex or the  $\delta$  subunit on the  $\text{Ca}^{2+}$  channel  $\alpha_1$  subunit. Transient transfection of tsA201 cells with the cardiac L-type  $\alpha_{1C}$  subunit alone resulted in the expression of inward voltage-activated currents as well as measurable [<sup>3</sup>H]-PN200-110 binding to membranes from transfected cells. Coexpression of the  $\alpha_2\delta$  subunit significantly increased the macroscopic current amplitude, altered the voltage dependence and the kinetics of the current, and enhanced [<sup>3</sup>H]-PN200-110 binding. Except for the increase in amplitude, coexpression of the  $\delta$  subunit reproduced entirely the effects of the full-length  $\alpha_2\delta$  subunit on the biophysical properties of the  $\alpha_{1C}$  currents. However, no effect on specific [<sup>3</sup>H]-PN200-110 binding was observed on  $\delta$  subunit coexpression.

Likewise, profound effects on current kinetics of the neuronal  $\alpha_{1A}$  subunit were observed on coexpression of the  $\alpha_2\delta$  complex in *Xenopus* oocytes. Furthermore, by using a chimeric strategy, we localized the region involved in this regulation to the transmembrane domain of the  $\delta$  subunit. These data strongly suggest that the molecular determinants involved in  $\alpha_2\delta$  regulation are conserved across L-type and non-L type  $\text{Ca}^{2+}$  channels. Taken together, our results indicate that the region of the  $\alpha_2\delta$  subunit involved in the modulation of the gating properties of the high voltage-activated calcium channels is localized in the  $\delta$  domain of the protein. In contrast, the level of membrane expression of functional channels relies on the presence of the  $\alpha_2$  domain of the  $\alpha_2\delta$  complex.

**Key words:** L-type Ca channel; P/Q-type Ca channels;  $\alpha_2\delta$  subunit;  $\delta$  subunit; transient expression; tsA201 cells; dihydropyridine binding

Voltage-gated  $\text{Ca}^{2+}$  channels are multisubunit protein complexes that control the entry of  $\text{Ca}^{2+}$  ions across the membrane of excitable cells and play a major role in several physiological processes, including neurotransmission, muscle contraction, hormone secretion, and gene expression. Five classes of voltage-gated  $\text{Ca}^{2+}$  channels have been described so far on the basis of their biophysical and pharmacological properties (T-, L-, N-, P/Q-, and R-types). Functional differences among  $\text{Ca}^{2+}$  channel types are attributable to several factors, including the expression of distinct  $\alpha_1$  pore-forming proteins and the selective association of  $\beta$  and  $\alpha_2\delta$  regulatory subunits (for review, see Catterall, 1995; Dunlap et al., 1995; De Waard et al., 1996).

According to available biochemical (Chang and Hosey, 1988; Schneider and Hofmann, 1988; Kuniyasu et al., 1992; Tokumaru et al., 1992) and molecular biological data (Mikami et al., 1989; Hullin et al., 1992; Perez-Reyes et al., 1992; Collin et al., 1993),  $\text{Ca}^{2+}$  channels are composed of at least three subunits:  $\alpha_1$ ,  $\beta$ , and

$\alpha_2\delta$ . Expression of the cloned  $\beta$  subunit results in an increase in current amplitude and changes the biophysical properties of the  $\alpha_1$  pore-forming subunit (Mori et al., 1991; Hullin et al., 1992; Perez-Reyes et al., 1992; Neely et al., 1993, 1995; Nishimura et al., 1993; Chien et al., 1995; Massa et al., 1995; Pérez-García et al., 1995; Kamp et al., 1996). Likewise, functional coexpression of the  $\alpha_2\delta$  subunit, the product of a single gene that is post-translationally processed to yield separate subunits ( $\alpha_2$  and  $\delta$ ) linked by disulfide bonds (De Jongh et al., 1990; Jay et al., 1991), also results in significantly increased macroscopic currents through  $\alpha_1/\beta$  recombinant calcium channels (Singer et al., 1991; Itagaki et al., 1992; Williams et al., 1992; Shistik et al., 1995; Bangalore et al., 1996; Wiser et al., 1996). Effects on dihydropyridine (DHP) binding also have been attributed to expression of the  $\beta$  and  $\alpha_2\delta$  auxiliary subunits (Welling et al., 1993; Mitterdorfer et al., 1994; Wei et al., 1995).

Although these studies suggest multiple roles for the  $\alpha_2\delta$  and  $\beta$  subunits in the processing and function of  $\text{Ca}^{2+}$  channels, little has been reported about the mechanisms of interaction between the  $\alpha_1$  and  $\alpha_2\delta$  subunits without the modulatory effect of the  $\beta$  subunits. Even less is known about the functional significance of the  $\delta$  subunit. To begin to address how these proteins participate in channel function, we have studied the regulatory effects of both the  $\alpha_2\delta$  ancillary complex and the  $\delta$  subunit on the cardiac L-type and the neuronal class A  $\alpha_1$  pore-forming subunits.

## MATERIALS AND METHODS

**Cell culture and transfection.** Human embryonic kidney tsA201 cells (HEK293 cells transformed with SV40 large T antigen) were grown in

Received April 29, 1997; revised June 9, 1997; accepted June 30, 1997.

R.F. is supported by a Human Frontier Science Program Organization postdoctoral fellowship. C.A.G. is supported by an American Heart Association predoctoral fellowship (Iowa affiliate). K.P.C. is an Investigator of the Howard Hughes Medical Institute. This work benefited from the use of the University of Iowa Diabetes and Endocrinology Research Center (National Institutes of Health DK25295). We thank Drs. X. Wei, T. P. Snutch, T. Tanabe, and L. Birnbaumer for providing the cDNA clones and Dr. A. George Jr for the tsA201 cell line. We are also grateful to H. Liu for experimental support and Drs. M. Henry and G. Biddlecome for helpful comments on this manuscript.

Correspondence should be addressed to Dr. Kevin P. Campbell, Howard Hughes Medical Institute, Department of Physiology and Biophysics, University of Iowa College of Medicine, 400 Eckstein Medical Research Building, Iowa City, IA 52242. Copyright © 1997 Society for Neuroscience 0270-6474/97/176884-08\$05.00/0

DMEM–high glucose supplemented with 10% equine serum, 2 mM L-glutamine, 110 mg/l sodium pyruvate, and 50  $\mu$ g/ml gentamycin at 37°C in a 5% CO<sub>2</sub> and 95% air humidified atmosphere. Transfections were performed with the calcium phosphate method (Ausubel et al., 1995) with 10  $\mu$ g of plasmid cDNA encoding the rabbit L-type Ca<sup>2+</sup> channel  $\alpha_{1C}$  pore-forming subunit (Wei et al., 1991) alone or in combination (molar ratio 1:1) with either plasmid cDNA encoding the rat full-length Ca<sup>2+</sup> channel  $\alpha_2\delta$  regulatory complex (Kim et al., 1992; Gurnett et al., 1996) or the  $\delta$  subunit alone (Gurnett et al., 1996). The plasmid cDNA-encoding  $\delta$  subunit was made by assembling a PCR fragment in the pcDNA3 mammalian expression plasmid (Invitrogen, San Diego, CA) after the  $\alpha_2\delta$  signal sequence. The  $\delta$ N-myc plasmid used in Western blot analysis was made by using two sequential PCR reactions and ligating the product into the *Kpn*I and *Eco*RI sites of the pcDNA3 vector. For electrophysiology, 3  $\mu$ g of a plasmid DNA encoding the CD8 surface marker (EBO-pcD-Leu2; American Type Culture Collection, Rockville, MD) also was added to the DNA transfection mixture to select cells that expressed Ca<sup>2+</sup> channels.

**Immunoblotting and in vitro translation.** tsA201 cells were harvested 2–3 d after transfection, and cell microsomes were prepared. Cells were lifted off plates into PBS, collected by centrifugation, and resuspended in lysis buffer (50 mM Tris-HCl, pH 7.4) in the presence of protease inhibitors (in  $\mu$ M): 0.8 aprotinin, 640 benzamidin, 1.1 leupeptin, 0.7 pepstatin A, and 230 PMSF. Cells were homogenized and centrifuged at 1300  $\times$  g for 5 min. The microsomes in the supernatant were collected by centrifugation at 130,000  $\times$  g for 37 min, resuspended in 0.3 M sucrose, 20 mM Tris, and protease inhibitors, and stored at –80°C. Subsequently, equivalent amounts (200  $\mu$ g of protein) of cell microsomes were electrophoresed on 5–16% gradient SDS-PAGE and transferred to nitrocellulose membranes. Membranes were incubated overnight with a polyclonal antibody against  $\alpha_2\delta$  (rabbit 136; 1:400) or a monoclonal antibody against the myc epitope (9E10; 1:1000), subsequently incubated with either horseradish peroxidase-conjugated goat anti-rabbit IgG or goat anti-mouse IgG (Boehringer Mannheim, Indianapolis, IN) at 1:1000, and visualized with ECL. Ca<sup>2+</sup> channel subunits also were synthesized by coupled *in vitro* transcription and translation with the TNT lysate system (Promega, Madison, WI) from the same plasmid cDNA used in transfections and analyzed by SDS-PAGE.

**Electrophysiology.** One day after transfection tsA201 cells were transferred to poly-L-lysine-coated coverslips and grown for 1–2 d until used for electrophysiology. To select Ca<sup>2+</sup> channel-expressing cells, we incubated a coverslip immediately before recording in bathing solution (see below) containing 1–2  $\times$  10<sup>6</sup>/ml paramagnetic beads precoated with a monoclonal antibody (ITI-5C2) specific for the CD8 membrane antigen (DynaL, Lake Success, NY), and the positively transfected cells were subjected to the whole-cell mode of the patch-clamp technique (Hamill et al., 1981). Briefly, patch pipettes were pulled from borosilicate glass capillaries. Typical pipette resistances were 2–5 M $\Omega$  when filled with internal solution. Currents were recorded with an Axopatch 200A amplifier (Axon Instruments, Foster City, CA) and acquired on-line, using a TL-1 interface with pClamp 6 software (Axon). After the whole-cell mode had been established, capacitive transients were canceled with the amplifier. Currents were obtained from a holding potential of –80 mV by applying test pulses every 20 sec, and data were leak-subtracted on-line by a standard P/4 protocol. Current signals were filtered at 1–2 kHz (internal four-pole Bessel filter) and digitized at 20 or 1.67 kHz, depending on the duration of the voltage steps. The bath solution contained (in mM): 40 BaCl<sub>2</sub>, 125 TEA-Cl, 10 HEPES, and 5 glucose, pH 7.3. The internal solution consisted of (in mM): 135 CsCl, 5 MgCl<sub>2</sub>, 10 EGTA, 10 HEPES, 4 Mg-ATP, and 0.1 GTP, pH 7.3.

Electrophysiological analysis of calcium currents expressed in *Xenopus* oocytes was performed as described previously (De Waard and Campbell, 1995). Briefly, the follicle membranes of stage V and VI isolated *Xenopus laevis* oocytes were digested enzymatically with 2 mg/ml collagenase IA (Sigma, St. Louis, MO) to facilitate injection and recording. cRNAs were transcribed *in vitro*, using T7 RNA polymerase or SP6 RNA polymerase in the case of  $\alpha_{1A}$ . Oocytes were injected with 50 nl of various subunit composition at the following cRNA concentrations: 0.7  $\mu$ g/ $\mu$ l  $\alpha_{1A}$ , 0.1  $\mu$ g/ $\mu$ l  $\beta_4$ , and 0.7  $\mu$ g/ $\mu$ l full-length  $\alpha_2\delta$  subunit or  $\alpha_2$ Ad chimeric construct (Gurnett et al., 1996). Currents were recorded by the two-electrode voltage-clamp method with a TEV-200 amplifier (Dagan, Minneapolis, MN). Both voltage and current electrodes were filled with 3 M KCl and had resistances of  $\sim$ 0.5 M $\Omega$ . Peak Ba<sup>2+</sup> currents were measured for a test potential of 0 mV from a holding potential of –90 mV. Recordings were filtered at 0.5 kHz, sampled at 5 kHz, and analyzed

by pClamp 6. Leak and capacitance currents were subtracted on-line by a P/6 protocol. The bath solution contained (in mM): 40 Ba(OH)<sub>2</sub>, 50 NaOH, 2 KCl, 1 niflumic acid, 0.1 EGTA, and 5 HEPES, pH 7.4.

**Radioligand binding.** The effect of the Ca<sup>2+</sup> channel auxiliary subunits on the dihydropyridine binding of the  $\alpha_{1C}$ -transfected cells was characterized as follows. Aliquots (80  $\mu$ g of protein) of cell microsomes prepared as mentioned above were resuspended in a total volume of 400  $\mu$ l of buffer A (50 mM Tris, 0.1% BSA, and protease inhibitors) and incubated with increasing concentrations of (+)-[methyl-<sup>3</sup>H]-PN200-110 (Amersham, Arlington Heights, IL) in the dark at 37°C. After 60 min the receptor–ligand complexes were collected and washed with buffer A on Whatman GF/B filters with a cell harvester. Nonspecific binding was determined by the addition of 50  $\mu$ M nitrendipine 10–15 min before the addition of [<sup>3</sup>H]-PN200-110. Specific binding was calculated by subtracting nonspecific from total binding.

**Statistical analysis.** The data are given as mean  $\pm$  SE, and the number of experiments is indicated in the figure legends. Statistical differences between two means were determined by Student's *t* tests. Means were considered significantly different when *p* < 0.05.

## RESULTS

### *In vitro* transcription–translation and cell expression of Ca<sup>2+</sup> channel subunits

The plasmids used in the transfection initially were examined via a cell-free transcription–translation system. The  $\alpha_{1C}$ ,  $\alpha_2\delta$ , and  $\delta$  cDNA clones directed the synthesis of three polypeptides of the expected molecular weight. Likewise, the expression of the  $\alpha_2\delta$  complex and the  $\delta$  subunit (containing the myc epitope fused to its N terminus) was demonstrated in tsA201 cells 48 hr post-transfection by Western blot analysis with either an antibody against the  $\alpha_2$  protein or the anti-myc antibody, respectively (data not shown). The expression of the  $\alpha_{1C}$  subunit (the pore-forming and DHP-sensitive component of the channel) was detected by electrophysiology and binding experiments, as detailed below.

### Effect of the regulatory subunits on current amplitude

We initiated the study of the regulatory effects of the  $\alpha_2\delta$  complex on the L-type Ca<sup>2+</sup> channel by comparing the fundamental biophysical properties between cells transiently transfected with constructs encoding  $\alpha_{1C}$  alone or cotransfected with the  $\alpha_2\delta$  or  $\delta$  subunits. Figure 1*A* shows representative examples of mean current traces (average of three successive sweeps) obtained during 150 msec pulses in untransfected (control) and transfected cells at a test potential of +30 mV. The top trace reveals the absence of endogenous voltage-activated Ca<sup>2+</sup> channels in control cells. In contrast, transfection with the Ca<sup>2+</sup> channel  $\alpha_{1C}$  subunit resulted in the expression of inward voltage-activated currents both in the presence and absence of the auxiliary subunits. A large increase in current amplitude was observed on coexpression of the full-length  $\alpha_2\delta$  subunit: the peak current amplitude was increased approximately threefold at +30 mV (Fig. 1*B*, Table 1). Although coexpression of the  $\delta$  subunit did not modify the magnitude of the  $\alpha_{1C}$  currents, evident changes in voltage dependence and waveform were observed (see below).

### Effect of the auxiliary subunits on the voltage dependence of the expressed currents

Previous studies in our laboratory with neuronal class A recombinant Ca<sup>2+</sup> channels expressed in *Xenopus* oocytes demonstrated that coexpression of the  $\delta$  subunit did not result in an enhancement of current amplitude (Gurnett et al., 1996). The question was raised, however, whether this protein directly interacted with the  $\alpha_1$  subunit although it had no effect on the one parameter studied (current amplitude). In the present study a direct comparison of the electrophysiological properties of singly transfected and cotransfected cells showed that the concomitant

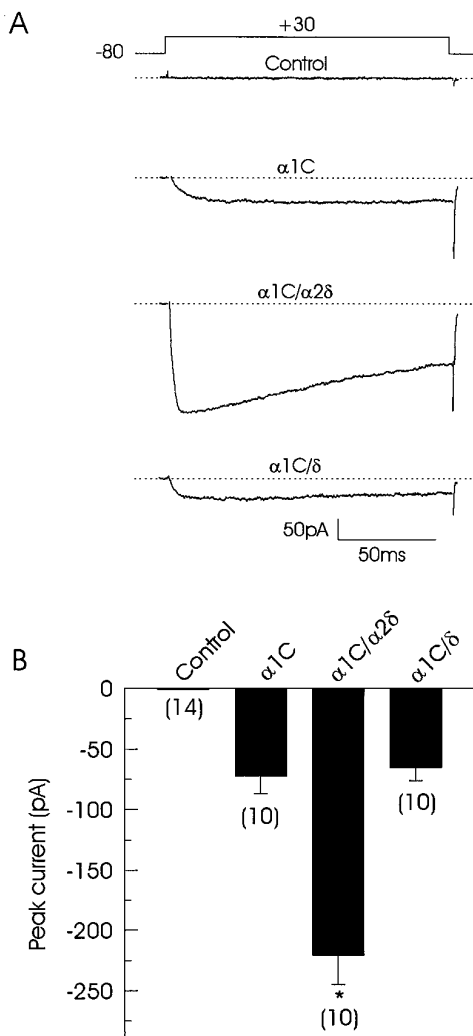


**Table 1. Differential effects of  $\alpha_2\delta$  and  $\delta$  on the biophysical and binding properties of the  $\alpha_{1C}$  currents**

\* Currents were recorded during depolarizations from  $-80$  to  $+30$  mV.  
 $B_{\text{max}}$ , Maximum binding capacity;  $K_D$ , dissociation constant (mean  $\pm$  SE;  $n = 3-5$ ).

test potential of  $+30$  mV. Figure 2B shows that the inactivation of the  $\alpha_{1C}$  currents occurs at relatively depolarized holding potentials; this has been reported also for other expressed high-voltage-activated channels (De Waard and Campbell, 1995). More importantly, coexpression of either  $\alpha_2\delta$  or  $\delta$  regulatory subunits induced a  $\sim 10$  mV hyperpolarizing shift in the voltage for 50% steady-state inactivation (Table 1).

**Effect of the auxiliary subunits on current kinetics**  
 We also investigated whether other properties of the expressed channels such as the inactivation kinetics could be modified by the presence of the regulatory subunits. Hence, the effect of the  $\alpha_2\delta$  and  $\delta$  subunits on inactivation was estimated from the percentage of current remaining after 150 msec activating pulses (Fig. 3A). The presence of either regulatory subunit decreased significantly the percentage of the remaining current at the end of the depolarizing pulse, indicating that both  $\alpha_2\delta$  and  $\delta$  subunits were able to accelerate inactivation of the  $\alpha_{1C}$  currents.

#### Effect of the auxiliary subunits on current kinetics

To analyze this action in more detail, we estimated voltage-dependent inactivation from the time course of the currents during 1 sec activating pulses to  $+20$  mV by fitting the decaying component with a single exponential equation. The use of Ba<sup>2+</sup> as the charge carrier in these experiments minimized any Ca<sup>2+</sup>-dependent inactivation. Traces in Figure 3B exemplify normalized representative records of membrane currents in singly transfected and cotransfected cells and show that variation in channel subunit composition results in different inactivation behavior. The decay of the macroscopic currents recorded from cells expressing  $\alpha_{1C}$  is slow as compared with those produced by coexpression of  $\alpha_{1C}$  with either the full-length  $\alpha_2\delta$  subunit or the  $\delta$  subunit. Figure 3C compares the time constants of the currents expressed as a function of the step voltage and clearly indicates that the currents induced in the presence of the regulatory subunits inactivate faster than the currents recorded in cells transfected with only the  $\alpha_{1C}$  subunit.

To test the individual contribution of the  $\alpha_2$  and the  $\delta$  domains on the inactivation kinetics of the macroscopic currents and to determine whether the molecular determinants involved in the  $\alpha_2\delta$  subunit regulation were conserved across L-type and non-L-type Ca<sup>2+</sup> channels, we performed additional electrophysiological

**Figure 1.** Whole-cell currents in tsA201 transiently transfected cells. *A*, Ba<sup>2+</sup> currents induced by activating pulses in four different representative cells. *Top trace* corresponds to the current recorded in a control (untransfected) cell. *Lower traces* correspond to current records that were obtained in cells transfected with Ca<sup>2+</sup> channel subunits in various combinations. The voltage protocol is shown above the traces, and the dotted line represents the baseline current. *B*, Comparison of peak current amplitudes at  $+30$  mV in control and transfected cells. Data are expressed as mean  $\pm$  SE, and the number of recorded cells is indicated in parentheses. Statistical significance of the difference between singly transfected and cotransfected cells was determined by Student's *t* test (\* $p < 0.05$ ).

expression of  $\alpha_2\delta$  not only increased current amplitude but also influenced the voltage dependence of activation and inactivation. This allowed us then to study the effect of the  $\delta$  subunit on these properties. As illustrated in Figure 2A, in cells transfected with  $\alpha_{1C}$  only, the current begins to turn on at  $-10$  mV and reaches the peak at  $+30$  mV. When the peak currents measured at each test potential were normalized to the maximum current observed in each cell, averaged and plotted as a function of test potential, a  $\sim 10$  mV shift in the  $I-V$  curve in the hyperpolarizing direction was observed in the cells that expressed the  $\alpha_2\delta$  subunit. Cotransfection of the  $\delta$  subunit resulted in a similar shift in the voltage dependence of activation (Table 1).

The development of steady-state inactivation was studied by holding the cells for 1.2 sec at potentials ranging successively from  $-80$  through  $+40$  mV before a 50 msec step depolarization to a

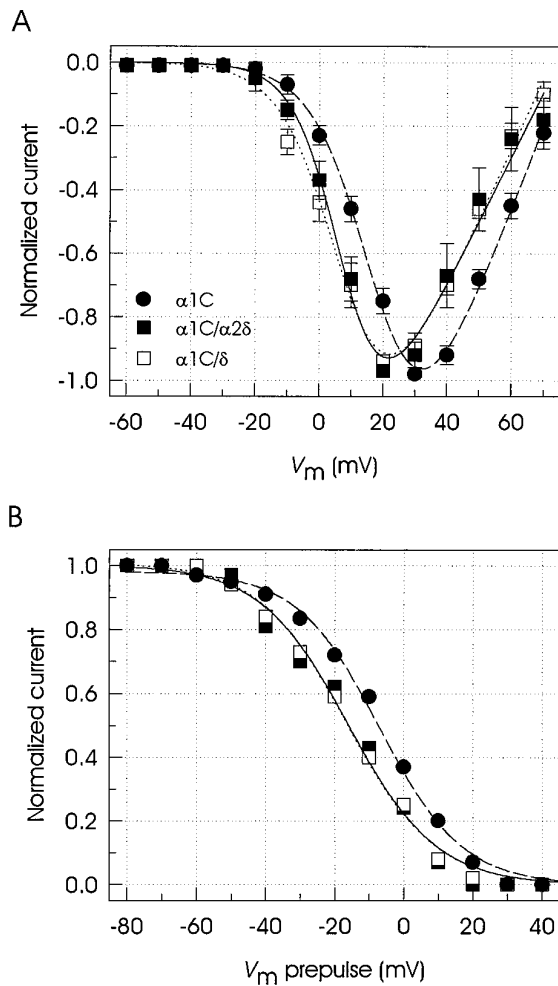


**Figure 2.** Voltage dependence of the currents through expressed Ca<sup>2+</sup> channels. *A*, Plot of peak normalized current–voltage relationships in transiently transfected cells. Currents were recorded in response to 150 msec depolarizations from a holding potential of  $-80$  mV with a 10 mV increase in the pulse amplitude per step. Symbols represent mean  $\pm$  SE values of five to eight cells in each condition. Fits of the  $I$ - $V$  curves were obtained assuming an activation curve of a Boltzmann type:  $I_{Ba} = [g(V_m - V_{rev})]/(1 + \exp[-(V_m - V_{1/2})/s])$ , where  $g$  is the conductance,  $V_m$  represents the test potential,  $V_{rev}$  is the apparent reversal potential, and  $s$  is the range of potential for an  $e$ -fold change around  $V_{1/2}$ . *B*, Measurement of the voltage dependence of inactivation at steady state. The graph shows peak currents at  $+30$  mV as a function of the prepulse potential for three different cells ( $\alpha_1C$ ,  $\bullet$ ;  $\alpha_1C/\alpha_2\delta$ ,  $\blacksquare$ ;  $\alpha_1C/\delta$ ,  $\square$ ). A series of 13 different 1.2 sec prepulse potentials from  $-80$  to  $+40$  mV was applied first, and the inactivated currents were measured with 50 msec test pulses. The obtained inactivation curves were fit with a Boltzmann function of the form:  $I_{Ba} = I_{max}/(1 + \exp[(V_m - V_{1/2})/s])$ , where the current amplitude  $I_{Ba}$  has decreased to a half-amplitude at  $V_{1/2}$  with an  $e$ -fold change over  $s$  mV. Pertinent parameters of the fits are given in Table 1.

cal recordings in *Xenopus* oocytes expressing the neuronal  $\alpha_{1A}$  subunit. Because the  $\alpha_2$  domain is completely extracellular (Gurnett et al., 1996; Wiser et al., 1996) and does not bind directly to the  $\alpha_1$  subunit in the absence of the  $\delta$  domain (Gurnett et al., 1997), the interaction between these two proteins is difficult to assess. To overcome this problem, we created an  $\alpha_2\delta$  chimeric subunit in which the transmembrane and the cytoplasmic regions of the  $\delta$  subunit were substituted by equivalent sequences of adhalin, an unrelated type I transmembrane protein ( $\alpha_2Ad$ ; Gurnett et al., 1996). This chimera has been shown to coimmunopre-

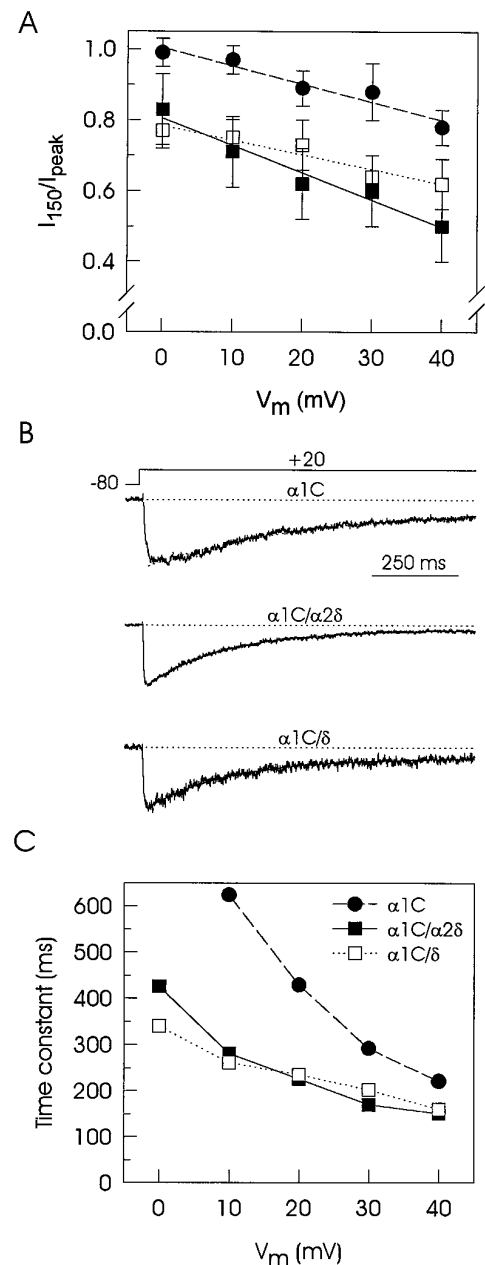


**Figure 3.** Effect of the  $\alpha_2\delta$  complex on inactivation kinetics in transiently transfected tsA201 cells. *A*, The percentage of current remaining 150 msec into the depolarizing pulse is plotted at various membrane potentials in  $\alpha_1C$  ( $\bullet$ ),  $\alpha_1C/\alpha_2\delta$  ( $\blacksquare$ ), and  $\alpha_1C/\delta$  ( $\square$ ) expressing cells. A straight line provided a close fit to these data, and although of no theoretical significance, it was used to emphasize differences between singly transfected and cotransfected cells ( $n = 10$ ). *B*, Representative records of currents obtained from three different transfected cells. The currents were recorded in response to 1 sec depolarizing pulses from  $-80$  to  $+20$  mV and ranged from  $-70$  to  $-150$  pA but are shown normalized to allow for comparison of kinetics. The inactivating phase of the currents was fit (superimposed lines) with a single exponential equation of the form:  $I_{Ba} = A\exp(-t/\tau) + c$ , where  $A$  is the initial amplitude,  $t$  is time,  $\tau$  is the time constant for inactivation, and  $c$  is a constant. *C*, Time constants of  $\alpha_1C$  currents are plotted at various membrane potentials. The same cells were used in *B* and *C* and represent typical values in each group ( $n = 3$  cells). Mean  $\pm$  SE values are given in Table 1.

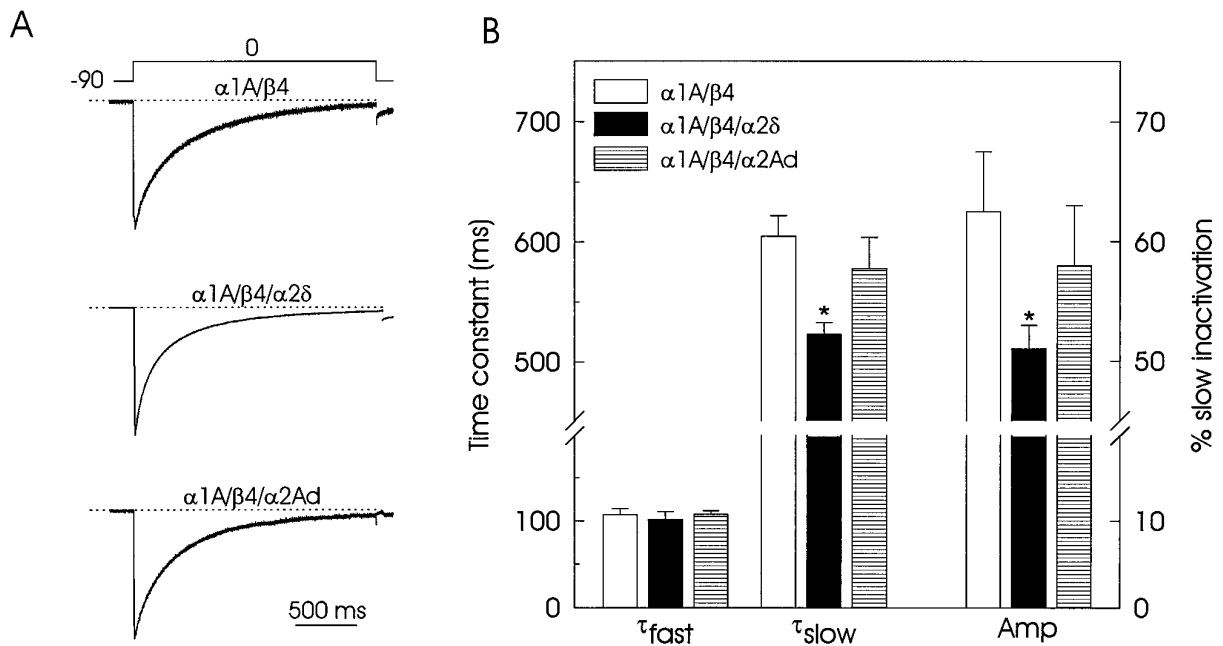


**Figure 4.** Time course of inactivation of the currents through recombinant calcium channels expressed in *Xenopus* oocytes. *A*, Normalized representative currents for oocytes coexpressing the  $\alpha_{1A}$  and the  $\beta_4$  subunits in the absence or in the presence of the full-length  $\alpha_2\delta$  or the chimeric  $\alpha_2Ad$  subunits. In all cases the decay of the currents was poorly fit by a single exponential. The sum of two exponential functions was necessary:  $I_{Ba} = I_{\infty} + A_f(\exp(-t/\tau_f) + A_s(\exp(-t/\tau_s) + c$ , where  $I_{\infty}$  is the steady-state inward current,  $A$  is the amplitude,  $t$  is time, and  $\tau_f$  and  $\tau_s$  are time constants for the fast and slow components, respectively. *B*, Pooled data comparing the average time constants ( $\tau_{fast}$  and  $\tau_{slow}$ ) and relative contribution of the slow component of inactivation amplitude (*Amp*) at 0 mV from various oocytes in the three groups ( $n = 6$ ). Asterisks denote significant differences ( $p < 0.05$ ).

cipitate with the  $\alpha_1$  subunit (Gurnett et al., 1997) and allowed us to test the participation of the  $\alpha_2$  and the  $\delta$  domains on the acceleration of the inactivation rate of the  $\alpha_1$  expressed currents.

In agreement with previous electrophysiological studies in *Xenopus* oocytes (Mori et al., 1991; Williams et al., 1992; Ellinor et al., 1993), we observed that expression of the neuronal Ca<sup>2+</sup> channel  $\alpha_{1A}$  pore-forming subunit alone generally resulted in small current density, although high concentrations of Ba<sup>2+</sup> were used to increase the resolution of the currents. However, coexpression of the  $\beta_4$  subunit allowed us to increase the expression of the  $\alpha_{1A}$  subunit to levels that permitted a systematic characterization of the biophysical properties of inactivation as detailed below.

Figure 4*A* compares the time course of normalized representative traces during 2 sec depolarizing steps from  $-90$  to  $0$  mV recorded in oocytes injected with various subunit combinations:  $\alpha_{1A}/\beta_4$ ;  $\alpha_{1A}/\beta_4/\alpha_2\delta$ , and  $\alpha_{1A}/\beta_4/\alpha_2Ad$ . In the same manner as in tsA201 transfected cells, the  $\alpha_1$  currents in oocytes decayed during sustained depolarization as a result of the voltage-dependent inactivation of the channels. However, the time course of this inactivation consisted of two kinetic components: the first component followed a fast time constant and constituted  $\sim 35\%$  of the total inactivating current, and the second component was represented by a slower time constant and constituted the remaining  $\sim 65\%$ . As illustrated in Figure 4*B*, the average value of the time constant for the fast component ( $\tau_{fast}$ ) was approximately the same in the three sets of oocytes investigated. Conversely, the time constant for the slow component ( $\tau_{slow}$ ) was clearly faster in the  $\alpha_2\delta$  subunit-expressing oocytes than in the other two groups of cells. In addition, the amplitude of the slow component (*Amp*) also was reduced greatly in the oocytes injected with the  $\alpha_2\delta$  subunit. The expression of the chimera ( $\alpha_2Ad$ ) did not affect the

inactivation kinetics significantly, although there was a slight but not statistically significant reduction in both the time constant and the amplitude of the slow component of the current. These results suggest that the presence of an intact  $\delta$  domain, including transmembrane sequence, is necessary for the acceleration in the inactivation rate of the  $\alpha_1$  currents on  $\alpha_2\delta$  subunit expression.

### Modulation of the DHP binding

To characterize the DHP-binding affinity of the  $\alpha_{1C}$ -transfected cells and its possible modulation by the  $\alpha_2\delta$  subunit, we performed equilibrium radioligand binding experiments that used [<sup>3</sup>H]-PN200-110. In an initial series of experiments we observed that  $\alpha_{1C}$  currents were sensitive to micromolar concentrations of DHPs (data not shown). Accordingly, Figure 5*A* shows representative saturation isotherms of [<sup>3</sup>H]-PN200-110 binding to microsomes from  $\alpha_{1C}$ ,  $\alpha_{1C}/\alpha_2\delta$ , and  $\alpha_{1C}/\delta$ -coexpressing cells. Specific binding was not observed in untransfected cells, consistent with the absence of endogenous Ca<sup>2+</sup> currents and the absence of detectable levels of Ca<sup>2+</sup> channel subunit protein expression. Scatchard analysis of the [<sup>3</sup>H]-PN200-110 saturation binding data revealed very similar values for the apparent dissociation constant ( $K_D$ ) and the total number of binding sites ( $B_{max}$ ) on both singly transfected cells and cells coexpressing the  $\delta$  subunit. In marked contrast, when singly transfected cells and cells coexpressing the  $\alpha_2\delta$  subunit were compared, a significant increase in both the number of binding sites and in affinity for the drug was observed (Table 1).

To elucidate the mechanisms underlying the large  $\alpha_2\delta$ -induced increase in  $\alpha_{1C}$  current amplitude, we compared current amplitude and DHP binding in both singly transfected and cotransfected cells. Because DHPs bind to the  $\alpha_{1C}$  subunit, an increase in the number of binding sites could account for the increase in

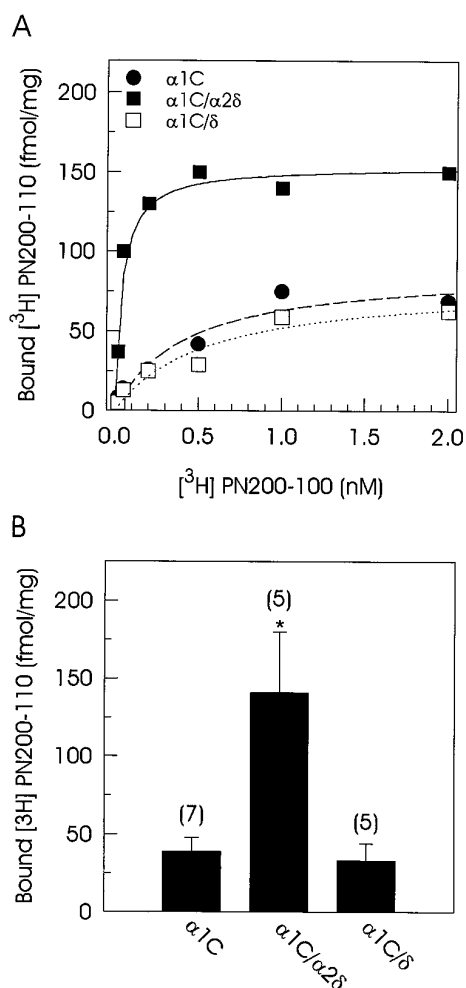


**Figure 5.** Dihydropyridine binding to the expressed Ca<sup>2+</sup> channels. *A*, Equilibrium binding curves for [<sup>3</sup>H]-PN200-110 in cells transfected with  $\alpha_{1C}$  alone or in combination with the  $\alpha_2\delta$  or the  $\delta$  subunits. Symbols represent mean values of specific DHP binding of duplicate samples in one representative experiment. Data were fit with a one-site ligand-binding equation of the form:  $y = [L] \cdot Cap / (K_D + [L])$ , where  $L$  is the concentration of free ligand,  $Cap$  is the maximum bound ligand, and  $K_D$  is the dissociation constant. *B*, Comparison of specific [<sup>3</sup>H]-PN200-110 binding to microsomes of tsA201 cells transfected with  $\alpha_{1C}$  alone or in combination with  $\alpha_2\delta$  or  $\delta$  subunits. Binding assays were performed with 1 nM [<sup>3</sup>H]-PN200-110. Data are given as mean  $\pm$  SE, and the number of separate experiments is indicated in parentheses. Asterisks denote significant differences ( $p < 0.05$ ).

current magnitude. Figure 5*B* shows the comparison of specific DHP binding to microsomes from tsA201 transfected cells, using a near-saturating concentration of [<sup>3</sup>H]-PN200-110 (1 nM). Coexpression of  $\alpha_2\delta$  subunit resulted in a  $\sim 3.6$ -fold increase in the amount of [<sup>3</sup>H]-PN200-110 binding. When it is compared with the approximately threefold increase in current amplitude seen by coexpression of the  $\alpha_2\delta$  subunit, this comparison suggests that there is an important correlation between the ability to increase current amplitude and the ability to enhance DHP binding. Consistent with this, the  $\delta$  subunit was incapable of increasing either the current amplitude or the DHP binding (Table 1).

## DISCUSSION

We have analyzed the effects induced by interaction of the  $\alpha_{1C}$  subunit with the  $\alpha_2\delta$  and  $\delta$  auxiliary subunits on the fundamental

biophysical properties of the recombinant channels. Our data clearly show that the  $\alpha_2\delta$  subunit significantly increased L-type calcium channel activity in transiently transfected tsA201 cells (Fig. 1). Likewise, as a result of this interaction, the  $\alpha_2\delta$  subunit induced a hyperpolarizing shift in activation and steady-state inactivation (Fig. 2) of the expressed channels. Interestingly, we found that the  $\delta$  subunit reproduced entirely the effects of the full-length  $\alpha_2\delta$  subunit on the voltage dependence of the macroscopic  $\alpha_{1C}$  currents. These findings therefore provide evidence that the  $\delta$  subunit per se can modulate the voltage-dependent behavior of the L-type Ca<sup>2+</sup> channel by interacting with the  $\alpha_{1C}$  subunit. Moreover, it may localize the region involved in modulation of voltage dependence to the  $\delta$  domain of the  $\alpha_2\delta$  complex such that the interaction between these two proteins may affect the S4 voltage sensor.

Another manifestation of the interaction between the  $\alpha_{1C}$  subunit with the regulatory subunits is the acceleration of the inactivation rate. The traces in Figure 3*B* show that, during depolarization, inward currents in transfected tsA201 cells spontaneously decay in external Ba<sup>2+</sup>, indicating that the expressed calcium channels undergo voltage-dependent inactivation. The time course of the decaying component of these currents is well described with a single exponential equation. We found that expression of the  $\alpha_2\delta$  subunit influenced the rate at which the currents inactivated. Again, the  $\delta$  domain completely reproduced the effect of the full-length  $\alpha_2\delta$  complex on inactivation kinetics (Table 1). Consistent with the above-mentioned findings, the percentage of decay of the  $\alpha_{1C}$  currents was increased significantly in the presence of either regulatory subunit when inactivation was estimated from the percentage of current remaining after 150 msec activating pulses (Fig. 3*A*, Table 1).

In contrast with the monoexponential decay of the currents in the transfected tsA201 cells, the Ca<sup>2+</sup> channels expressed in *Xenopus* oocytes inactivated in a biexponential manner (Fig. 4). Although many factors may give rise to two components, several experimental findings suggested to us that this result may reflect an intrinsic property of the neuronal expressed channels: the endogenous currents were negligible; the ratio of the slow and fast current amplitudes remained constant from oocyte to oocyte and was independent of the total current amplitude recorded. Moreover, our results indicate that the slow inactivating component of these currents was sensitive to the regulatory effect of the  $\alpha_2\delta$  subunit. However, coexpression of the  $\alpha_2Ad$  chimera, in which the transmembrane domain of the  $\alpha_2\delta$  complex ( $\delta$  subunit) was replaced with that of adhalin, did not modify the inactivation kinetics of the  $\alpha_{1A}/\beta_4$  channels. This suggests that the  $\delta$  transmembrane domain may be the primary moiety involved in this regulation. Interestingly, because the molecular determinants of voltage-dependent inactivation in Ca<sup>2+</sup> channels have been localized to the membrane-spanning segment S6 of the first repeat (IS6) of the  $\alpha_1$  subunit (Zhang et al., 1994), this region also may be involved in the interaction with the  $\delta$  subunit.

Another regulatory action of the  $\alpha_2\delta$  complex was the drastic increase in  $\alpha_{1C}$  current amplitude. The mechanisms underlying this action may be better understood by comparing current amplitude and DHP binding in both singly transfected and cotransfected cells. Our results demonstrated that the total number of DHP binding sites increased on coexpression of the  $\alpha_2\delta$  subunit. In addition, there was a large augmentation in the affinity for the DHP when  $\alpha_2\delta$  was present (Fig. 5, Table 1). These results confirm that the  $\alpha_2\delta$  subunit is crucial to the reconstitution of DHP binding (Wei et al., 1995), because the binding affinity and

number of binding sites approached that of rabbit cardiac microsomes (Nishimura et al., 1993; Wei et al., 1995) only when the  $\alpha_2\delta$  subunit was coexpressed. Furthermore, these observations suggest that the  $\alpha_2\delta$  complex acts primarily by inducing important conformational changes in the pore-forming subunit. These changes in  $\alpha_{1C}$  conformation then would be responsible for an increase not only in the accessibility of the drug to its site but also in the opening probability of the channel, as it has been observed in *Xenopus* oocytes (Shistik et al., 1995). Because the binding site for DHPs has been localized to the IIS5–S6 and IVS5–S6 regions (Grabner et al., 1996; Peterson et al., 1996), these sites also may have been involved in the interaction with the  $\alpha_2\delta$  complex.

An alternative possibility to explain the results could be that the conformational changes induced by the  $\alpha_2\delta$  complex may play an important role in the localization of the expressed channels on the cell surface. In support of this interpretation, Bangalore et al. (1996) have demonstrated that the coexpression of the  $\alpha_2\delta$  complex increases the number of functional L-type calcium channels in the cell membrane as gauged by gating charge movement. In addition, Shistik et al. (1995) have shown that the  $\alpha_2\delta$  complex triples the amount of  $\alpha_{1C}$  protein localized in the plasma membrane of *Xenopus* oocytes as detected by immunoprecipitation. As mentioned above, our results indicate that coexpression of the L-type calcium channel pore-forming subunit with  $\alpha_2\delta$  increased both the number of the total binding sites and the affinity for the radiolabeled PN200-110. In contrast, coexpression with the  $\delta$  subunit did not affect specific DHP binding (Fig. 5, Table 1). Interestingly, the chimeric  $\alpha_2\delta$  subunit has been shown to mimic the effects of the full-length  $\alpha_2\delta$  subunit on PN200-110 binding when expressed in tsA201 cells (Gurnett et al., 1997). These findings indicate not only that expression of the  $\alpha_2$  domain is necessary for the formation of a stable interaction capable of reconstituting normal DHP binding but also suggest that coexpression of this domain of the  $\alpha_2\delta$  protein may facilitate proper insertion of channel proteins into the cell membrane. The mechanisms of the  $\alpha_2$  subunit effect on the membrane trafficking of the  $\alpha_1$  subunit require further investigation. Gating current studies will be needed to examine this issue.

Taken together, our findings indicate that the  $\alpha_2\delta$  complex and the  $\delta$  subunit interact in specific ways with the  $\alpha_1$  subunit and participate in the functional regulation of the L-type and non-L-type calcium channels. Our previous studies indicated that the extracellular  $\alpha_2$  domain, which is particularly sensitive to structural modification, provides the elements required for channel stimulation (Gurnett et al., 1996). Here, we localize the region of the  $\alpha_2\delta$  subunit involved in the shift in voltage-dependent activation and steady-state inactivation as well as the acceleration of the inactivation kinetics to the  $\delta$  subunit, whereas the effects on increased currents and DHP binding affinity require the presence of the  $\alpha_2$  domain of the  $\alpha_2\delta$  complex.

## REFERENCES

- Ausubel FM, Brent R, Kingston RE, Moore DD, Seidman JG, Smith JA, Struhl K (1995) Current protocols in molecular biology. New York: Wiley.
- Bangalore R, Mehrke G, Gingrich K, Hofmann F, Kass RS (1996) Influence of L-type Ca channel  $\alpha_2\delta$  subunit on ionic and gating current in transiently transfected HEK293 cells. *Am J Physiol* 270:H1521–H1528.
- Catterall W (1995) Structure and function of voltage-gated ion channels. *Annu Rev Biochem* 64:493–531.
- Chang FC, Hosey MM (1988) Dihydropyridine and phenylalkylamine receptors associated with cardiac and skeletal muscle. *J Biol Chem* 263:18929–18937.
- Chien A, Zhao X, Shirokov RE, Puri TS, Chang CF, Sun D, Rios E, Hosey MM (1995) Roles of membrane-localized  $\beta$  subunit in the formation and targeting of functional L-type Ca<sup>2+</sup> channels. *J Biol Chem* 270:30036–30044.
- Collin T, Wang JJ, Nargeot J, Schwartz A (1993) Molecular cloning of three isoforms of the L-type voltage-dependent calcium channel  $\beta$  subunit from normal human heart. *Circ Res* 72:1337–1344.
- De Jongh KS, Warner C, Catterall WA (1990) Subunits of purified calcium channels:  $\alpha_2$  and  $\delta$  are encoded by same gene. *J Biol Chem* 265:14738–14741.
- De Waard M, Campbell KP (1995) Subunit regulation of the neuronal  $\alpha_{1A}$  Ca<sup>2+</sup> channel. *J Physiol (Lond)* 485:619–634.
- De Waard M, Gurnett CA, Campbell KP (1996) Structural and functional diversity of voltage-activated calcium channels. In: *Ion channels*, Vol IV (Narahashi T, ed), pp 41–87. New York: Plenum.
- Dunlap K, Luebke JI, Turner TJ (1995) Exocytotic Ca<sup>2+</sup> channels in mammalian central neurons. *Trends Neurosci* 18:89–98.
- Ellinor PT, Zhang JF, Randall AD, Zhou M, Schwarz TL, Tsien RW, Horne WA (1993) Functional expression of a rapidly inactivating neuronal calcium channel. *Nature* 363:455–458.
- Grabner M, Wang Z, Hering S, Streissnig J, Glossmann H (1996) Transfer of 1,4-dihydropyridine sensitivity from L-type to class A (BI) calcium channels. *Neuron* 16:207–218.
- Gurnett CA, De Waard M, Campbell KP (1996) Dual function of the voltage-dependent Ca<sup>2+</sup> channel  $\alpha_2\delta$  subunit in current stimulation and subunit interaction. *Neuron* 16:431–440.
- Gurnett CA, Felix R, Campbell KP (1997) Extracellular interaction of the voltage-dependent Ca<sup>2+</sup> channel  $\alpha_2\delta$  and  $\alpha_1$  subunits. *J Biol Chem* 272:18508–18512.
- Hamill OP, Marty A, Neher E, Sakmann B, Sigworth FJ (1981) Improved patch-clamp techniques for high-resolution current recording from cells and cell-free membrane patches. *Pflügers Arch* 391:85–100.
- Hullin R, Singer-Lahat D, Freichel M, Biel M, Dascal N, Hofmann F, Flockerzi V (1992) Calcium channel  $\beta$  subunit heterogeneity: functional expression of cloned cDNA from heart, aorta, and brain. *EMBO J* 11:885–890.
- Itagaki K, Koch WJ, Bodi I, Klockner U, Slish DF, Schwartz A (1992) Native-type DHP-sensitive calcium channel currents are produced by cloned rat aortic smooth muscle and cardiac  $\alpha_1$  subunits expressed in *Xenopus laevis* oocytes and are regulated by  $\alpha_2$ - and  $\beta$ -subunits. *FEBS Lett* 297:221–225.
- Jay SD, Sharp AH, Kahl SD, Vedvick TS, Harpold MM, Campbell KP (1991) Structural characterization of the dihydropyridine-sensitive calcium channel  $\alpha_2$ -subunit and the associated  $\delta$  peptides. *J Biol Chem* 266:3287–3293.
- Kamp JT, Pérez-García MT, Marban E (1996) Enhancement of ionic current and charge movement by coexpression of calcium channel  $\beta_{1A}$  subunit with  $\alpha_1$  subunit in a human embryonic kidney cell line. *J Physiol (Lond)* 492:89–96.
- Kim HL, Kim H, Lee P, King RG, Ching H (1992) Rat brain expresses an alternatively spliced form of the dihydropyridine-sensitive L-type calcium channel  $\alpha_2$  subunit. *Proc Natl Acad Sci USA* 89:3251–3255.
- Kuniyasu A, Oca K, Ide-Yamada T, Hatanaka Y, Abe T, Nakayama H, Kanaoka Y (1992) Structural characterization of the dihydropyridine receptor-linked calcium channel from porcine heart. *J Biochem* 112:235–242.
- Massa E, Kelly KL, Yule DI, MacDonald RL, Uhler MD (1995) Comparison of fura-2 imaging and electrophysiological analysis of murine calcium channel  $\alpha_1$  subunits coexpressed with novel  $\beta_2$  subunit isoforms. *Mol Pharmacol* 47:707–716.
- Mikami A, Imoto K, Tanabe T, Niidome T, Mori Y, Takeshima H, Narumiya S, Numa S (1989) Primary structure and functional expression of the cardiac dihydropyridine-sensitive calcium channel. *Nature* 340:230–233.
- Mitterdorfer J, Froschmayr M, Grabner M, Striessnig J, Glossmann H (1994) Calcium channels: the  $\beta$ -subunit increases the affinity of dihydropyridine and Ca<sup>2+</sup> binding sites of the  $\alpha_1$ -subunit. *FEBS Lett* 352:141–145.
- Mori Y, Friedrich T, Kim MS, Mikami A, Nakai J, Ruth P, Bosse E, Hofmann F, Flockerzi V, Furuichi T, Mikoshiba K, Imoto K, Tanabe T, Numa S (1991) Primary structure and functional expression from complementary DNA of a brain calcium channel. *Nature* 350:398–402.
- Neely A, Wei X, Olcese R, Birnbaumer L, Stefani E (1993) Potentiation

- by the  $\beta$  subunit of the ratio of ionic current to the charge movement in the cardiac calcium channel. *Science* 262:575–578.
- Neely A, Olcese R, Baldelli P, Wei X, Birnbaumer L, Stefani E (1995) Dual activation of the cardiac Ca<sup>2+</sup> channel  $\alpha_{1C}$  subunit and its modulation by the  $\beta$  subunit. *Am J Physiol* 268:C732–C740.
- Nishimura S, Takeshima H, Hofmann F, Flockerzi V, Imoto K (1993) Requirement of the calcium channel  $\beta$  subunit for functional conformation. *FEBS Lett* 324:283–286.
- Pérez-García MT, Kamp TJ, Marban E (1995) Functional properties of cardiac L-type calcium channels transiently expressed in HEK293 cells. Roles of  $\alpha_1$  and  $\beta$  subunits. *J Gen Physiol* 105:289–306.
- Perez-Reyes E, Castellano A, Kim HS, Bertrand P, Baggstrom E, Lacerda AE, Wei XY, Birnbaumer L (1992) Cloning and expression of a cardiac/brain  $\beta$  subunit of the L-type calcium channel. *J Biol Chem* 267:1792–1797.
- Peterson BZ, Tanada TN, Catterall WA (1996) Molecular determinants of high-affinity dihydropyridine binding in L-type calcium channels. *J Biol Chem* 271:5293–5296.
- Schneider T, Hofmann F (1988) The bovine cardiac receptor for calcium channel blockers is a 195 kDa protein. *Eur J Biochem* 174:369–375.
- Shistik E, Ivanina T, Puri T, Hosey M, Dascal N (1995) Ca<sup>2+</sup> current enhancement by  $\alpha_2/\delta$  and  $\beta$  subunits in *Xenopus* oocytes: contributions of changes in channel gating and  $\alpha_1$  protein level. *J Physiol (Lond)* 489:55–62.
- Singer D, Biel M, Lotan I, Flockerzi V, Hoffmann F, Dascal N (1991) The roles of the subunits in the function of the calcium channel. *Science* 253:1553–1557.
- Tokumaru H, Anzai K, Abe T, Kirino Y (1992) Purification of the cardiac 1,4-dihydropyridine receptor using immunoaffinity chromatography with a monoclonal antibody against the  $\alpha_2\delta$  subunit of the skeletal muscle dihydropyridine receptor. *Eur J Pharmacol* 227:363–370.
- Wei X, Perez-Reyes E, Lacerda AE, Schuster G, Brown AM, Birnbaumer L (1991) Heterologous regulation of the cardiac Ca<sup>2+</sup> channel  $\alpha_1$  subunit by skeletal muscle  $\beta$  and  $\gamma$  subunits. *J Biol Chem* 266:21943–21947.
- Wei X, Pan S, Lang W, Kim H, Schneider T, Perez-Reyes E, Birnbaumer L (1995) Molecular determinants of cardiac Ca<sup>2+</sup> channel pharmacology. Subunit requirement for the high affinity and allosteric regulation of dihydropyridine binding. *J Biol Chem* 270:27106–27111.
- Welling A, Bosse E, Cavalié A, Bottlender R, Ludwig A, Nastainczyk W, Flockerzi V, Hoffmann F (1993) Stable co-expression of calcium channel  $\alpha_1$ ,  $\beta$ , and  $\alpha_2/\delta$  subunits in a somatic cell line. *J Physiol (Lond)* 471:749–765.
- Williams ME, Feldman DH, McCue AF, Brenner R, Velicelebi G, Ellis SB, Harpold MM (1992) Structure and functional expression of  $\alpha_1$ ,  $\alpha_2$ , and  $\beta$  subunits of a novel human neuronal calcium channel subtype. *Neuron* 8:71–84.
- Wiser O, Trus M, Tobi D, Halevi S, Giladi E, Atlas D (1996) The  $\alpha_2/\delta$  subunit of voltage-sensitive Ca<sup>2+</sup> channels is a single transmembrane extracellular protein which is involved in regulated secretion. *FEBS Lett* 379:15–20.
- Zhang JF, Ellinor PT, Aldrich RW, Tsien RW (1994) Molecular determinants of voltage-dependent inactivation in calcium channels. *Nature* 372:97–100.